receptor antagonism. Gastroenterology **134** : 2004-2013, 2008
11) 上園保仁：がん患者の症状緩和に役立つ漢方薬―漢方薬の有効性を示す，臨床につながる基礎研究―．がん患者と対療 **22** : 140-146, 2011
12) Fujitsuka N, Asakawa A, Uezono Y, et al : Potentiation of ghrelin signaling attenuates cancer anorexia-cachexia and prolongs survival. Transl Psychiatry **1** : e23, 2011
13) Sadakane C, Muto S, Nakagawa K, et al : 10-Gingerol, a component of rikkunshito, improves cisplatin-induced anorexia by inhibiting acylated ghrelin degradation. Biochem Biophys Res Commun **412** : 506-511, 2011
14) Uezono Y, Miyano K, Sudo Y, et al : A review of traditional Japanese medicines and their potential mechanism of action. Curr Pharm Des **18** : 4839-4853, 2012

Am J Physiol Endocrinol Metab 306: E373–E387, 2014.
First published December 17, 2013; doi:10.1152/ajpendo.00116.2013.

New cancer cachexia rat model generated by implantation of a peritoneal dissemination-derived human stomach cancer cell line

Kiyoshi Terawaki,[1,5] Yumi Sawada,[1] Yohei Kashiwase,[1,3] Hirofumi Hashimoto,[4] Mitsuhiro Yoshimura,[4] Masami Suzuki,[1] Kanako Miyano,[1] Yuka Sudo,[1,3] Seiji Shiraishi,[1] Yoshikazu Higami,[3] Kazuyoshi Yanagihara,[2] Yoshio Kase,[5] Yoichi Ueta,[4] and Yasuhito Uezono[1]

[1]Division of Cancer Pathophysiology, National Cancer Center Research Institute, Tokyo, Japan; [2]Division of Translational Research, Exploratory Oncology Research and Clinical Trial Center, National Cancer Center Hospital East, Kashiwa, Japan; [3]Laboratory of Molecular Pathology and Metabolic Disease, Faculty of Pharmaceutical Sciences, Tokyo University of Science, Chiba, Japan; [4]Department of Physiology, School of Medicine, University of Occupational and Environmental Health, Kitakyushu, Japan; [5]Tsumura Research Laboratories, Tsumura & Co., Ibaraki, Japan

Submitted 1 March 2013; accepted in final form 5 December 2013

Terawaki K, Sawada Y, Kashiwase Y, Hashimoto H, Yoshimura M, Suzuki M, Miyano K, Sudo Y, Shiraishi S, Higami Y, Yanagihara K, Kase Y, Ueta Y, Uezono Y. New cancer cachexia rat model generated by implantation of a peritoneal dissemination-derived human stomach cancer cell line. *Am J Physiol Endocrinol Metab* 306: E373–E387, 2014. First published December 17, 2013; doi:10.1152/ajpendo.00116.2013.—Cancer cachexia (CC), a syndrome characterized by anorexia and body weight loss due to low fat-free mass levels, including reduced musculature, markedly worsens patient quality of life. Although stomach cancer patients have the highest incidence of cachexia, few experimental models for the study of stomach CC have been established. Herein, we developed stomach CC animal models using nude rats subcutaneously implanted with two novel cell lines, i.e., MKN45c185, established from the human stomach cancer cell line MKN-45, and 85As2, derived from peritoneal dissemination of orthotopically implanted MKN45c185 cells in mice. Both CC models showed marked weight loss, anorexia, reduced musculature and muscle strength, increased inflammatory markers, and low plasma albumin levels; however, CC developed earlier and was more severe in rats implanted with 85As2 than in those implanted with MKN45cl85. Moreover, human leukemia inhibitory factor (LIF), a known cachectic factor, and hypothalamic orexigenic peptide mRNA levels increased in the models, whereas hypothalamic anorexigenic peptide mRNA levels decreased. Surgical removal of the tumor not only abolished cachexia symptoms but also reduced plasma LIF levels to below detectable limits. Importantly, oral administration of rikkunshito, a traditional Japanese medicine, substantially ameliorated CC-related anorexia and body composition changes. In summary, our novel peritoneal dissemination-derived 85As2 rat model developed severe cachexia, possibly caused by LIF from cancer cells, that was ameliorated by rikkunshito. This model should provide a useful tool for further study into the mechanisms and treatment of stomach CC.

cachexia; leukemia inhibitory factor; rikkunshito; stomach cancer model; anorexia

CANCER CACHEXIA, A MULTIFACTORIAL SYNDROME characterized by anorexia and the loss of body weight, adipose tissue, and skeletal muscle, is observed in 80% of advanced cancer patients and accounts for at least 20% of cancer-related deaths (20, 35, 42). This syndrome causes not only poor quality of life (QOL) but also poor responses to chemotherapy, highlighting the need for improved cancer cachexia treatments. Weight loss, the most prominent clinical feature of cachexia, is observed in 30–80% of cancer patients, depending on tumor type. For example, weight loss occurs at a very high frequency (83%) in stomach and pancreatic cancer patients but is less prominent in patients with breast cancer, acute nonlymphocytic leukemia, and sarcomas (35). Although cachexia strongly impacts the success of therapeutic treatments, the mechanisms underlying this syndrome are not fully understood. Stomach cancer patients in particular have the highest incidence of cachexia; however, few experimental models for the study of stomach cancer cachexia have been established (4, 14, 66).

A useful cachexia model must meet three of the following five diagnostic criteria in addition to weight loss: anorexia, decreased muscle strength, fatigue, low fat-free mass (FFM) index, and abnormal biochemistry (anemia, increased inflammatory markers, and low serum albumin) (14). Moreover, Argilés et al. (1) reported that two specific indicators, anorexia and metabolic disturbances, should be identified before arriving at a diagnosis of cachexia-associated weight loss. Although body weight maintenance is the most important end point of any cachexia treatment, body composition and QOL should also be monitored (1). Accordingly, anorexia and body composition are very important in both the diagnosis and treatment of cachexia and should be present in any experimental model designed to study this syndrome.

To address the need for an experimental stomach cancer cachexia animal model, we previously screened 15 human stomach cancer cell lines for their ability to induce weight loss in mice after subcutaneous implantation (63). Among the cell lines that were screened, only the MKN-45 cell line induced body weight loss, with an incidence of 40% in tumor-bearing mice (63). On the basis of these findings, we established two novel cell lines from MKN-45 cells: MKN45cl85 and 85As2 (63). Implantation of MKN45cl85 cells induces body weight loss in mice with 100% efficiency. The 85As2 cell line, derived from peritoneal metastasis of orthotopically implanted MKN45cl85 cells, has a strong capacity to induce peritoneal dissemination and body weight loss (100% efficiency) in mice.

Anorexia is a key factor in both the diagnosis and treatment of cachexia. Appetite facilitation reinforces physical strength and improves QOL. Thus, anorexia is very important for the evaluation of cachexia. In our previous mouse model, evaluation of cachexia based on weight loss was possible, whereas anorexia could not be used to assess cachexia because of instability in the reduction of food consumption (63). There-

Address for reprint requests and other correspondence: K. Terawaki, Div. of Cancer Pathophysiology, National Cancer Center Research Institute, 5-1-1 Tsukiji, Chuo-ku, Tokyo 104-0045, Japan (e-mail: kterawak@ncc.go.jp).

fore, our mouse cachexia model was not suitable to evaluate drug efficacy or mechanisms of cachexia-associated anorexia. To address this problem, we aimed to establish two novel stomach cancer cachexia models by implanting MKN45cl85 and 85As2 cell lines into nude rats. We determined the usefulness of these cancer cachexia models in evaluating anorexia, body composition changes (including low FFM), and weight loss. Moreover, body composition changes, including low FFM, are useful in elucidating the mechanisms of anorexia associated with stomach cancer cachexia. To investigate the underlying mechanisms of cachexia in these models, plasma levels of cytokines known to be involved in cancer cachexia development, such as interleukin (IL)-1, IL-6, tumor necrosis factor (TNF)α, and leukemia inhibitory factor (LIF) (13, 19, 40, 58), were also evaluated. Because the hypothalamus is a key regulator of energy homeostasis and a major site for the integration of metabolic signals in the central nervous system, the expression of hypothalamic feeding-regulating peptides was determined. In addition, the expression of the muscle-specific E3 ubiquitin ligases atrogin-1/muscle atrophy F-box (MAFbx) and muscle RING finger 1 (MuRF-1), which are important mediators of skeletal muscle loss, was also evaluated (6, 25).

To assess the efficacy of our novel stomach cancer cachexia rat models in evaluating treatment outcomes, we examined the impact of rikkunshito therapy on cachexia-associated symptoms in these models. Rikkunshito has been approved by the Ministry of Health, Labor, and Welfare of Japan and is widely prescribed as a remedy for various gastrointestinal syndromes, such as anorexia, dyspepsia, and gastritis (29, 44). Rikkunshito was found to improve anorexia symptoms in a double-blind study of patients with functional dyspepsia (29). Additionally, increasing evidence from experimental animal models has shown that rikkunshito ameliorates several types of anorexia (23, 24, 57). It has been reported that with rikkushito there is an increase in the secretion of the orexigenic hormone ghrelin by the inhibition of 5-HT2B/2C receptors, an enhancement of ghrelin receptor (GHSR) signaling efficiency, and a facilitation of gastric emptying and gastric adaptive relaxation, all of which may contribute to ameliorate anorexia (24, 32, 57, 60, 64). Herein, we examined specifically the efficacy of rikkunshito in ameliorating anorexia symptoms in our novel cancer cachexia rat models.

MATERIALS AND METHODS

Animal experimentation. Six-week-old male F344/NJcl-rnu/rnu rats (Clea-Japan, Tokyo, Japan) were housed individually under a 12:12-h light-dark cycle (lights on at 0800) at a constant temperature and humidity, with ad libitum access to food and water. Rats were allowed to acclimate to laboratory conditions for 2 wk prior to experimentation. All studies were performed according to the Guidelines for Animal Experiments drafted by the Committee for Ethics in Animal Experimentation of the National Cancer Center and approved by the committee (approval nos. T09-050-M02 and T09-050-C04), and they met the ethical standards required by the law and the guidelines concerning experimental animals in Japan.

Cell lines and culture conditions. MKN45cl85 and 85As2 cell lines were established from the human stomach MKN-45 cancer cell line, as described previously (63). Cells were maintained in RPMI 1640 medium (Nacalai Tesque, Kyoto, Japan) supplemented with 10% fetal bovine serum (Invitrogen, Carlsbad, CA), 100 IU/ml penicillin G sodium, and 100 μg/ml streptomycin sulfate (Nacalai Tesque) under a 5% CO_2 and 95% air atmosphere at 37°C.

Tumor cell implantation. MKN45cl85 and 85As2 cells were harvested from subconfluent cultures after brief exposure to 0.25% trypsin and 0.2% ethylenediaminetetraacetic acid. Cells were washed once in serum-free medium and resuspended in phosphate-buffered saline. Anesthetized rats were subcutaneously inoculated with either 1×10^6-10^7 cells/site (tumor-bearing rats) or saline alone (non-tumor-bearing control rats) in the left and right flanks. The major and minor tumor axes were measured, and the tumor volume was estimated using the following equation: tumor volume (cm^3) = major axis (cm) × minor axis (cm) × minor axis (cm) × 1/2, and tumor volume was converted to tumor weight (mg)/mm^3 (14, 17, 66).

Rat model characterization. Body weight and composition, organ tissue weight, food and water consumption, and grip strength were evaluated in each model. Body weight and food and water consumption were measured weekly. Body composition was determined using the ImpediVET Bioimpedance Spectroscopy device (ImpediMed, Brisbane, Australia) to accurately measure FFM, fat mass (FM), and total body water (TBW) (52). Blood collected from the abdominal aorta was centrifuged (3,000 rpm, 10 min), and the plasma was stored at −80°C until analysis. Organ tissues were immediately dissected and weighed. Gastrocnemius muscle tissue was fixed with 10% formalin and embedded in paraffin for histological analysis. Cross sectional area, perimeter, Feret diameter, and minimum Feret diameter were calculated using Image J software (15). Grip strength was measured using a grip strength meter for rats and mice (MK-380CM/F; Muromachi Kikai, Tokyo, Japan).

Tumor removal experiment. Anesthetized rats were subcutaneously inoculated with either 85As2 1×10^7 cells/site (tumor-bearing rats) or saline alone (non-tumor-bearing control rats) in the left and right flanks. Tumor growth, body weight, and food and water intake were measured weekly. Cancer cachexia clearly developed in tumor-bearing rats 2 wk after implantation. After that, tumor-bearing cancer cachectic rats were divided into two groups; one group was not treated and the other group had their tumors removed. Tumors were removed with surgical scissors, and the incision was closed using a surgical needle and sutures under anesthesia. The body composition was measured at *weeks 0* (before tumor implantation), *2* (before tumor removal), and *4* and *5* (after tumor removal). Grip strength was measured, and the plasma and gastrocnemius muscle were collected 5 wk after implantation.

Real-time polymerase chain reaction. Real-time polymerase chain reaction (PCR) was performed as described previously (56). Briefly, the hypothalamic area was dissected on an ice-cold metal plate, and total RNA was isolated using an Isogen kit (Nippon Gene, Tokyo, Japan) according to the manufacturer's instructions. First-strand cDNA was reverse transcribed from 5 μg of total RNA using the SuperScript First-Strand Synthesis System (Invitrogen, Carlsbad, CA) in a final volume of 100 μl. Diluted cDNA (2 μl) was amplified in a rapid thermal cycler (LightCycler; Roche Diagnostics, Barcelona, Spain) using LightCycler 480 SYBR Green I Mastermix (Roche, Barcelona, Spain) and the following primers: atrogin-1/MAFbx 5′-GAA GAC CGG CTA CTG TGG AA-3′ (forward) and 5′-ATC AAT CGC TTG CGG ATC T-3′ (reverse), MuRF-1 5′-AGG ACT CCT GCC GAG TGA C-3′ (forward) and 5′-TTG TGG CTC AGT TCC TCC TT-3′ (reverse), forkhead box O1 (Foxo-1) 5′-TCA GGC TAG GAG TTA GTG AGC A-3′ (forward) and 5′-AAG GAG GGG TGA AGG GCA TC-3′(reverse), Foxo-3 5′-CTC AGC CAG TGG ACA GTG AA-3′ (forward) and 5′-GCT CTG GAG TAG GGA TGC TG-3′ (reverse), Foxo-4 5′-GCC GAG CCT GTC CTT ATC CA-3′ (forward) and 5′-TTG AGT GTG TGA CCA CCT ATC CCT A-3′(reverse), IGF-I 5′-GCA CTC TGC TTG CTC ACC TTT A-3′ (forward) and 5′-TCC GAA TGC TGG AGC CAT A-3′ (reverse), and glyceraldehyde-3-phosphate dehydrogenase 5′-CCC CCA ATG TAT CCG TTG TG-3′ (forward) and 5′-TAG CCC AGG ATG CCC TTT AGT-3′ (reverse). PCR products were quantified using Light-

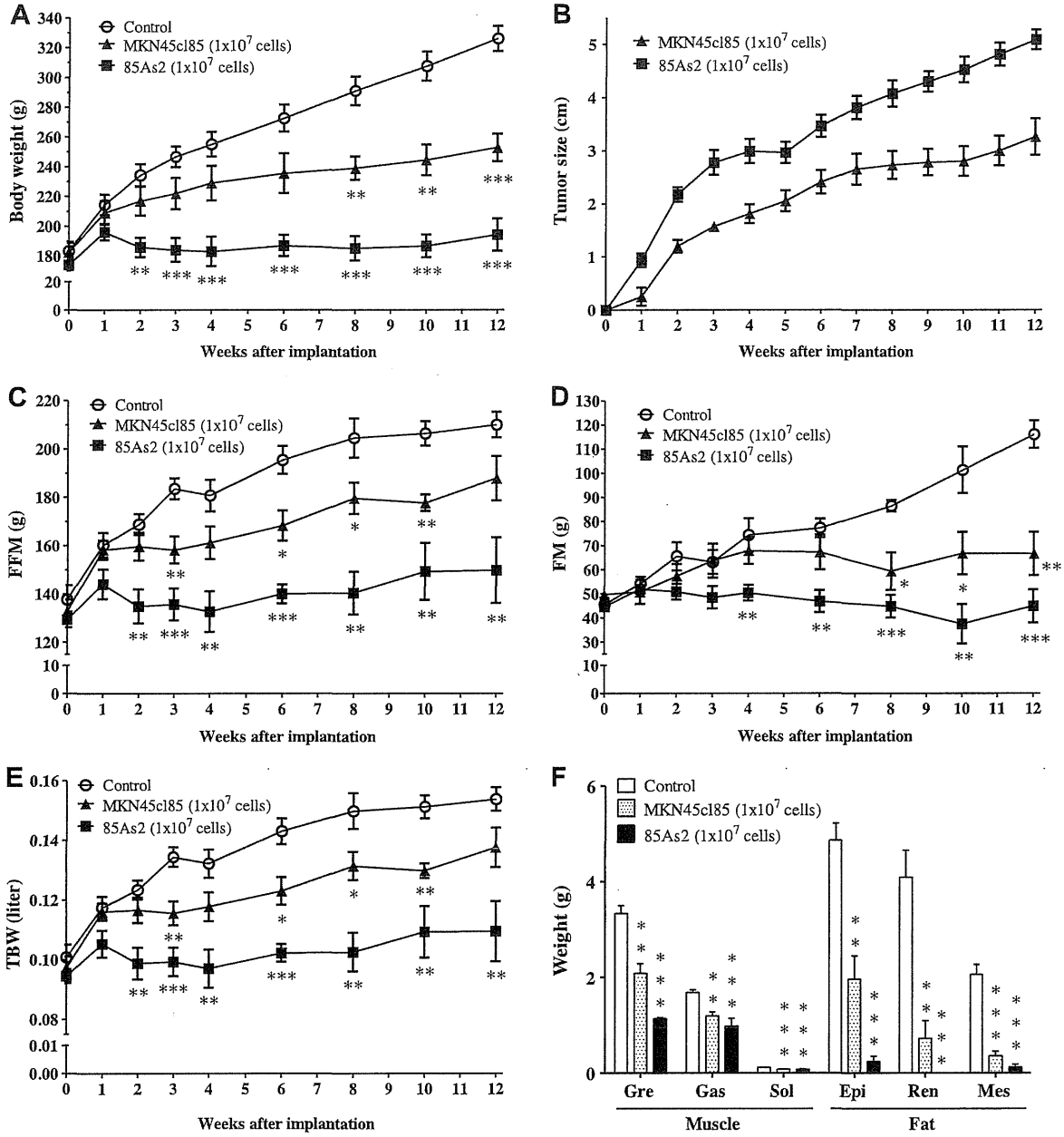

Fig. 1. Effects of MKN45cl85 and 85As2 cell implantation on body weight (*A*), tumor size (*B*), fat-free mass (FFM; *C*), fat mass (FM; *D*), total body water (TBW; *E*), and muscle and adipose tissue weights in nude rats (*F*). Rats were inoculated subcutaneously (sc) with MKN45cl85 or 85As2 cells in both flanks (1×10^7 cells/each site) at *week 0*. Rats inoculated with saline served as a control group. Each data point or bar represents the mean ± SE of 4–5 rats. Differences between groups were evaluated using Student's *t*-test or Welch's *t*-test. $^*P < 0.05$, $^{**}P < 0.01$, $^{***}P < 0.001$ vs. the control group. Gre, greater pectoral muscle; Gas, gastrocnemius muscle; Sol, soleus muscle; Epi, epididymal fat; Ren, perirenal fat; Mes, mesentery fat.

Cycler 480 software to analyze the exponential phase of amplification and the melting curve as recommended by the manufacturer. The amount of target mRNA in the experimental group relative to that in the control group was determined from the resulting fluorescence and threshold values (C_T) using the $2^{-\Delta\Delta C_T}$ method (37).

Cytokine measurements. Plasma levels of human IL-1β, IL-6, IL-8, TNFα, and LIF were measured using the Luminex Multiplex Assay (Affymetrix, Billerica, MA) (18). Rat IL-1β, IL-6, TNFα, keratinocyte-derived chemokine (KC), and interferon (IFN)γ plasma levels were measured using the Procarta Cytokine Assay Kit (Affymetrix). Plasma α1-acid glycoprotein and albumin levels were measured using a rat α1-acid glycoprotein enzyme-linked immunosorbent assay (ELISA) kit (Immunology Consultants Laboratory, Newberg, OR) and a rat albumin ELISA kit (Shibayagi, Gunma, Japan), respectively. Human cytokine levels were also measured in MKN45cl85 and 85As2 cell culture supernatants (5×10^5 cells/well) at 24 and 48 h.

In situ hybridization. In situ hybridization was performed as described previously (55). Briefly, frozen 12-μm-thick coronal brain sections were prepared in a cryostat at −20°C, thawed, and mounted onto gelatin/chrome alum-coated slides. The paraventricular nucleus

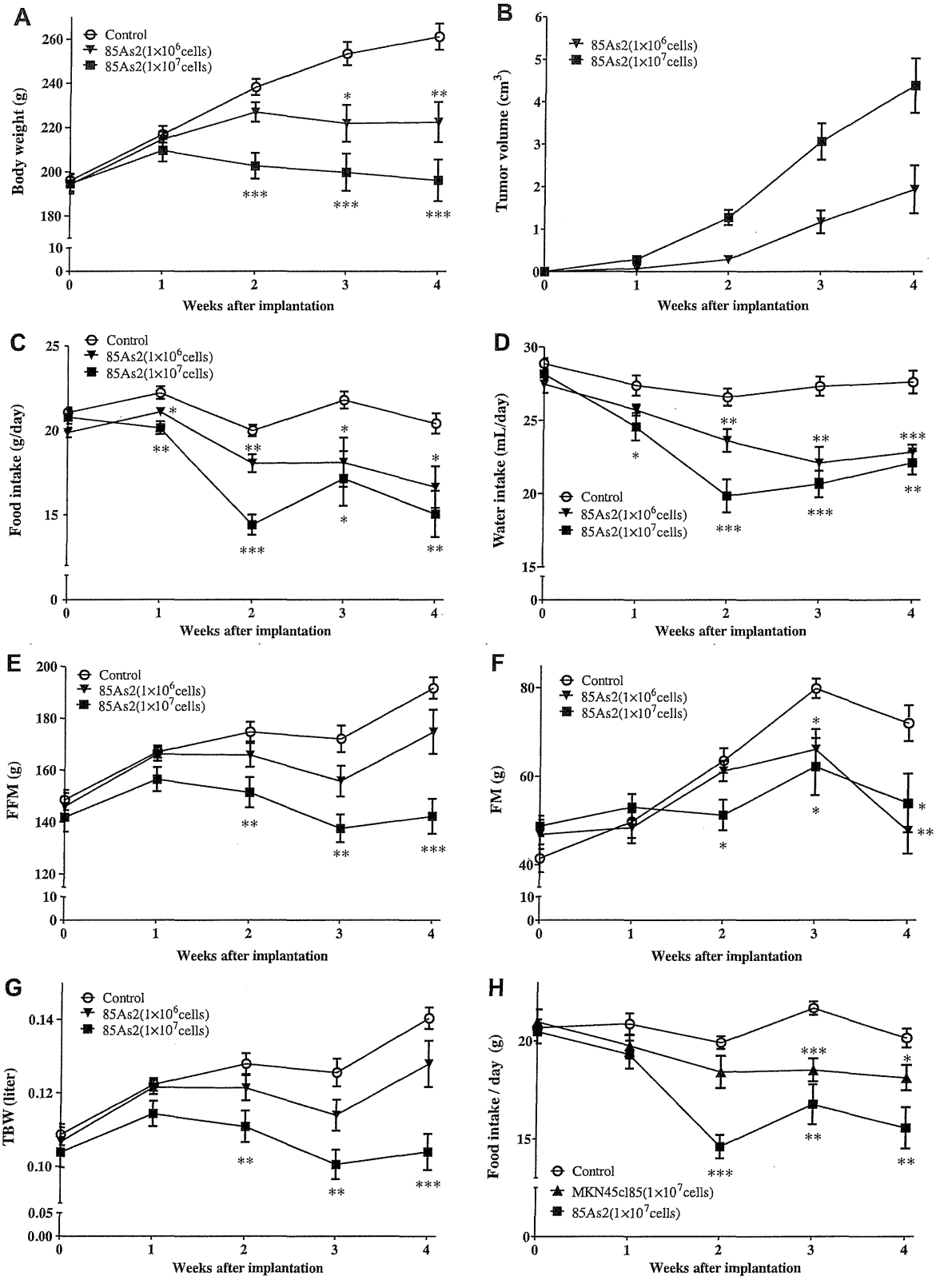
A
Body weight (g)
Control
85As2(1×10^6cells)
85As2(1×10^7cells)
Weeks after implantation
B
Tumor volume (cm^3)
85As2(1×10^6cells)
85As2(1×10^7cells)
Weeks after implantation
C
Food intake (g/day)
Control
85As2(1×10^6cells)
85As2(1×10^7cells)
Weeks after implantation
D
Water intake (mL/day)
Control
85As2(1×10^6cells)
85As2(1×10^7cells)
Weeks after implantation
E
FFM (g)
Control
85As2(1×10^6cells)
85As2(1×10^7cells)
Weeks after implantation
F
FM (g)
Control
85As2(1×10^6cells)
85As2(1×10^7cells)
Weeks after implantation
G
TBW (liter)
Control
85As2(1×10^6cells)
85As2(1×10^7cells)
Weeks after implantation
H
Food intake / day (g)
Control
MKN45cl85(1×10^7cells)
85As2(1×10^7cells)
Weeks after implantation

Table 1. *Body, tumor, muscle, fat, and organ weights in nude rats 4 wk after implantation with different 85As2 cell concentrations*

	Control	85As2 Cells	
		1×10^6	1×10^7
TW	0.00 ± 0.00	5.19 ± 1.54*	11.00 ± 2.31***,#
TV	0.00 ± 0.00	3.77 ± 1.27**	8.75 ± 1.50***,##
BW	259.62 ± 5.84	219.78 ± 8.98**	192.96 ± 8.62***
%control	100.0 ± 2.3	84.7 ± 3.5***	74.3 ± 3.3***
BW − CTW	259.62 ± 5.84	216.01 ± 10.18**	184.20 ± 9.25***,#
%control	100.0 ± 2.3	83.2 ± 3.9***	71.0 ± 3.6***,#
BW − TW	259.62 ± 5.84	214.59 ± 10.39***	181.96 ± 9.91***
%control	100.0 ± 2.3	82.7 ± 4.0***	70.1 ± 3.8***
Peak BW		226.89 ± 6.06	206.63 ± 7.15
%peak BW		94.4 ± 2.7	88.0 ± 3.5†
Muscle weights			
Greater pectoral	2.67 ± 0.11	1.88 ± 0.10***	1.42 ± 0.04***,##
Gastrocnemius	1.37 ± 0.04	1.17 ± 0.04***	0.97 ± 0.06***,##
Tibialis	0.54 ± 0.02	0.42 ± 0.03***	0.41 ± 0.04**
Soleus	0.08 ± 0.01	0.07 ± 0.00*	0.07 ± 0.01*
Fat weights			
Epididymis	3.78 ± 0.19	2.73 ± 0.36*	1.79 ± 0.30***
Perirenal	2.58 ± 0.28	1.53 ± 0.45	0.64 ± 0.34**
Mesentery	1.41 ± 0.13	0.95 ± 0.29	0.40 ± 0.18**
Organ weights			
Liver	10.36 ± 0.33	7.69 ± 0.56**	6.69 ± 0.31***
Spleen	0.63 ± 0.03	0.48 ± 0.02**	0.49 ± 0.03**

Data are expressed as the mean ± SE of 5 rats; all weight data are expressed in g. TW, tumor weight; TV, tumor volume; BW, body weight; CTW, converted tumor weight. Rats were implanted subcutaneously with either 85As2 cells (1×10^6 or 1×10^7 cells/site) or saline alone in both flanks. TV was estimated using the following equation: TV (cm^3) = major axis (cm) × minor axis (cm) × minor axis (cm) × 1/2, and the TV was converted to tumor weight (mg)/mm^3. TW and TV are expressed as the total for both sites. Values for bilateral tissues represent the mean of those for the 2 unilateral tissues. BW comparisons between the control group and 85As2 groups at 4 wk after implantation showed the following relationship: %control (%) = BW of each 85As2 group/BW of control group × 100. BW comparisons between peak BW and BW at 4 wk after implantation in each 85As2 group showed the following relationship: %peak body weight (%) = BW (− TW) at 4 wk after implantation/peak BW (− CTW) × 100. Differences between groups were evaluated using Student's *t*-test. Differences in TW and TV between the control group and 85As2 groups were evaluated using the Kruskal-Wallis test, followed by a post hoc Dunn's multiple comparison test. *$P < 0.05$, **$P < 0.01$, and ***$P < 0.001$ vs. the control group; #$P < 0.05$ and ##$P < 0.01$ vs. the 85As2 cell 1×10^6 cell group; †$P < 0.05$ vs. each peak BW.

(PVN), arcuate nucleus (ARC), and lateral hypothalamic area (LHA) were identified according to the Paxinos and Watson (48) atlas and confirmed by microscopy. Hybridization was conducted under a Nescofilm coverslip (Bando Chemical, Osaka, Japan). [^{35}S]3′-end-labeled deoxyoligonucleotides complementary to transcripts coding for neuropeptide Y (*NPY*; 5′-GGA GTA GTA TCT GGC CAT GTC CTC TGC TGG CGC GTC-3′), agouti-related protein (*AgRP*; 5′-CGA CGC GGA GAA CGA GAC TCG CGG TTC TGT GGA TCT AGC ACC TCT GCC-3′), proopiomelanocortin (*POMC*; 5′-CTT CTT GCC CAG CGG CTT GCC CCA GCA GAA GTG CTC CAT GGA CTA GGA-3′), cocaine- and amphetamine-regulated transcript (*CART*; 5′-TGG GGA CTT GGC CGT ACT TCT TCT CAT AGA TCG GAA TGC-3′), orexin (5′-TTC GTA GAG ACG GCA GGA ACA CGT CTT CTG GCG ACA-3′), corticotropin-releasing hormone (*CRH*; 5′-CAG TTT CCT GTT GCT GTG AGC TTG CTG AGC TAA CTG CTC TGC CCT GGC-3′), and melanin-concentrating hormone (*MCH*; 5′-CCA ACA GGG TCG GTA GAC TCG TCC CAG CAT-3′) were used as gene-specific probes (28, 30, 31, 43, 62). Total counts of 6×10^5 counts·min^{-1}·slide^{-1} for NPY, AgPR, POMC, CART, MCH, and CRH and 4×10^5 counts·min^{-1}·slide^{-1} for orexin were used. Hybridized sections containing the ARC, LHA, and PVN regions were exposed to autoradiography film (Hyperfilm; Amersham, Buckinghamshire, UK) for 4 days for orexin and 7 days for NPY, AgRP, POMC, CART, MCH, and CRH. Autoradiographic images were captured at ×40 magnification and quantified using an MCID imaging analyzer (Imaging Research, St. Catherines, ON, Canada). The images were captured by a charge-coupled device camera (Dage-MTI, Michigan City, IN). Mean absorbance was measured and compared with simultaneously exposed ^{14}C microscale samples (Amersham). The standard curve was fitted according to the absorbance of the ^{14}C microscale on the same film.

Respiratory metabolism. Oxygen consumption was measured with an O_2/CO_2 metabolism-measuring system (MK-5000RQ; Muromachi Kikai, Tokyo, Japan) (33, 45). Each rat was kept unrestrained in a sealed chamber with an airflow of 0.5 l/min at 25°C for 20 h without food. Air was sampled every 3 min, and oxygen consumption ($\dot{V}O_2$) and carbon dioxide production ($\dot{V}CO_2$) were calculated (ml·min^{-1}·kg^{-1}). Locomotor activity was measured simultaneously with an attached device. The respiratory quotient (RQ) was calculated by dividing $\dot{V}CO_2$ by $\dot{V}O_2$. Metabolic calories (E) were calculated using the system software as follows: E (cal·min^{-1}·kg^{-1}) = (1.07 × RQ + 3.98) × $\dot{V}O_2$/body weight.

Palliative therapeutic studies using rikkunshito. Rikkunshito was manufactured by Tsumura (Tokyo, Japan) by spray-drying a hot water

Fig. 2. Effects of 85As2 cell implantation at different concentrations on body weight (*A*), tumor volume (*B*), food intake (*C*), water intake (*D*), FFM (*E*), FM (*F*), and TBW (*G*) in nude rats. Rats were inoculated sc with 85As2 cells (1×10^6 or 1×10^7 cells/each site) or saline (control) in both flanks at *week 0*. Each data point represents the mean ± SE of 5–10 rats (0–2 wk: 10 rats; 3–4 wk: 5 rats). *H*: food intake comparisons between the MKN45cl85 group and 85As2 groups ≤4 wk after implantation. Rats were inoculated sc with MKN45cl85 or 85As2 cells in both flanks (1×10^7 cells/each site) at *week 0*. Rats inoculated with saline served as a control group. Each data point represents the mean ± SE of 9–10 rats. Differences between groups were evaluated using Student's *t*-test or Welch's *t*-test. *$P < 0.05$, **$P < 0.01$, ***$P < 0.001$ vs. the control group.

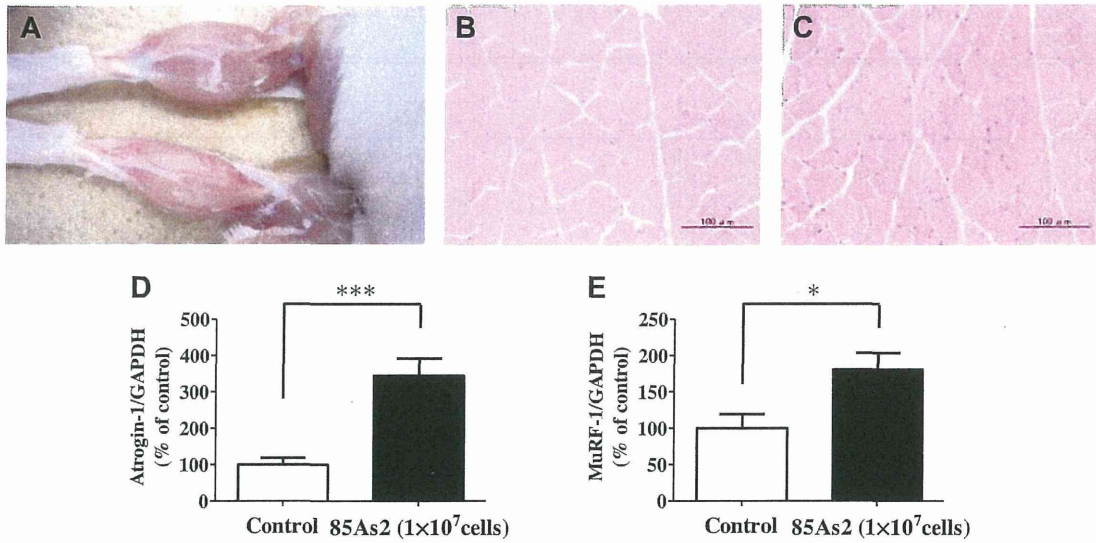

Fig. 3. Atrophy and expression of E3 ubiquitin ligases in the gastrocnemius muscle in 85As2-bearing cachectic rats 4 wk after implantation. Nude rats were inoculated subcutaneously with 85As2 cells (1×10^7 cells/each site) or saline (control) in both flanks at *week 0*. *A*: macroscopic observation of the gastrocnemius muscle in a control rat (*top* muscle in the photo) and cachectic rat (*bottom* muscle in the photo). *B* and *C*: histological observation of the gastrocnemius muscle tissue in a control rat (*B*) and cachectic rat (*C*). *D* and *E*: expression of the E3 ubiquitin ligases atrogin-1 (*D*) and muscle RING finger 1 (MuRF-1; *E*) in gastrocnemius muscle tissue. Each bar represents the mean ± SE of 7–8 rats. Differences between groups were evaluated using the Mann-Whitney *U*-test. $^*P < 0.05$ and $^{***}P < 0.001$ vs. the control group.

extract from the following eight crude drugs to form a powdered extract: *Atractylodis lanceae rhizoma* (4.0 g), *Ginseng radix* (4.0 g), *Pinelliae tuber* (4.0 g), *Hoelen* (4.0 g), *Zizyphi fructus* (2.0 g), *Aurantii nobilis pericarpium* (2.0 g), *Glycyrrhizae radix* (1.0 g), and *Zingiberis rhizoma* (0.5 g). The powdered rikkunshito extract was obtained from Tsumura. For oral administration into the stomach using a disposable sonde, rikkunshito was dissolved in distilled water (DW) at 10 g/ml in our laboratory. Rats were implanted subcutaneously (sc) with 85As2 cells in both flanks (1×10^7 cells/each site) on *day −14*. Rats inoculated with saline served as the non-tumor-bearing

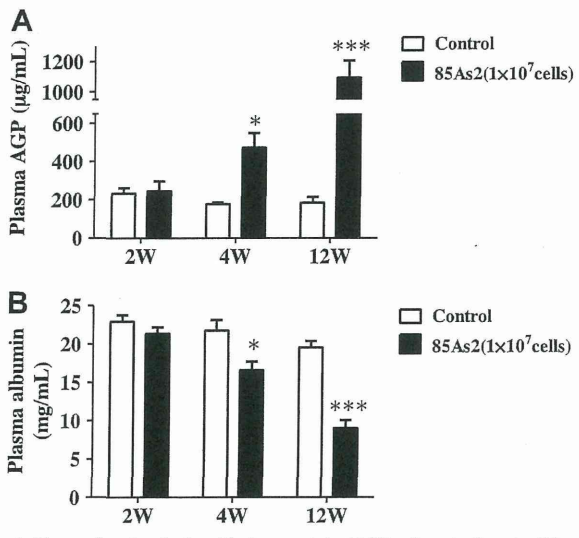

Fig. 4. Plasma levels of α1-acid glycoprotein (AGP; *A*) and albumin (*B*) at 2, 4, and 12 wk after 85As2 cell implantation in nude rats. Rats were inoculated sc with 85As2 cells (1×10^7 cells/each site) or saline (control) in both flanks at *week 0*. Each bar represents the mean ± SE of 5 rats. Differences between groups were evaluated using Student's *t*-test or Welch's *t*-test. $^*P < 0.05$ and $^{***}P < 0.001$ vs. the control group.

control group. Tumor-bearing rats were divided into two groups: a treatment (85As2 + rikkunshito) group and a tumor-bearing control (85As2 + DW) group. The treatment group was administered rikkunshito orally twice daily at 1,000 $mg \cdot kg^{-1} \cdot day^{-1}$ for 7 days (from *days 0* to *6*). The tumor-bearing control group was administered DW (10 ml/kg) over the same period. Non-tumor-bearing rats (control + DW group) were also administered DW over the same period. Tumor growth was measured weekly. Body weight and food and water intake were measured weekly until *day 0* and were measured daily thereafter. Food and water intake data after rikkunshito or DW administration are expressed as the daily, cumulative value from *days 0* to *7* or average value from *days 2* to *7*, and body weight data are expressed as body weight minus converted tumor weight. Body composition was measured on *days −14* (before tumor implantation), *0* (before administration), and *6* (after administration). Rats were anesthetized with isoflurane on *day 7*, and muscle and adipose tissues were immediately dissected and weighed.

Statistical analyses. All data are expressed as means ± SE. Differences between groups were evaluated using the Student's *t*-test, paired *t*-test, Welch's *t*-test, Mann-Whitney *U*-test, one-way analysis of variance followed by a post hoc Dunnett's multiple comparison test, or Kruskal-Wallis test followed by a post hoc Dunn's multiple comparison test. A *P* value of <0.05 was considered significant.

RESULTS

Implantation of MKN45cl85 and 85As2 cells induced cancer cachexia in rats. Subcutaneous implantation of either MKN45cl85 or 85As2 cells in rats induced progressive tumor growth beginning 1 wk after implantation and affected body weight and composition. Body weight was markedly reduced 2 wk after implantation of MKN45cl85 and 85As2 cells compared with controls, and thereafter, the differences gradually increased (Fig. 1, *A* and *B*). Additionally, all body composition parameters (FFM, FM, and TBW) were significantly lower in the MKN45cl85 and 85As2 groups than in the control group (Fig. 1, *C–E*). Moreover, all muscle and adipose tissue weights

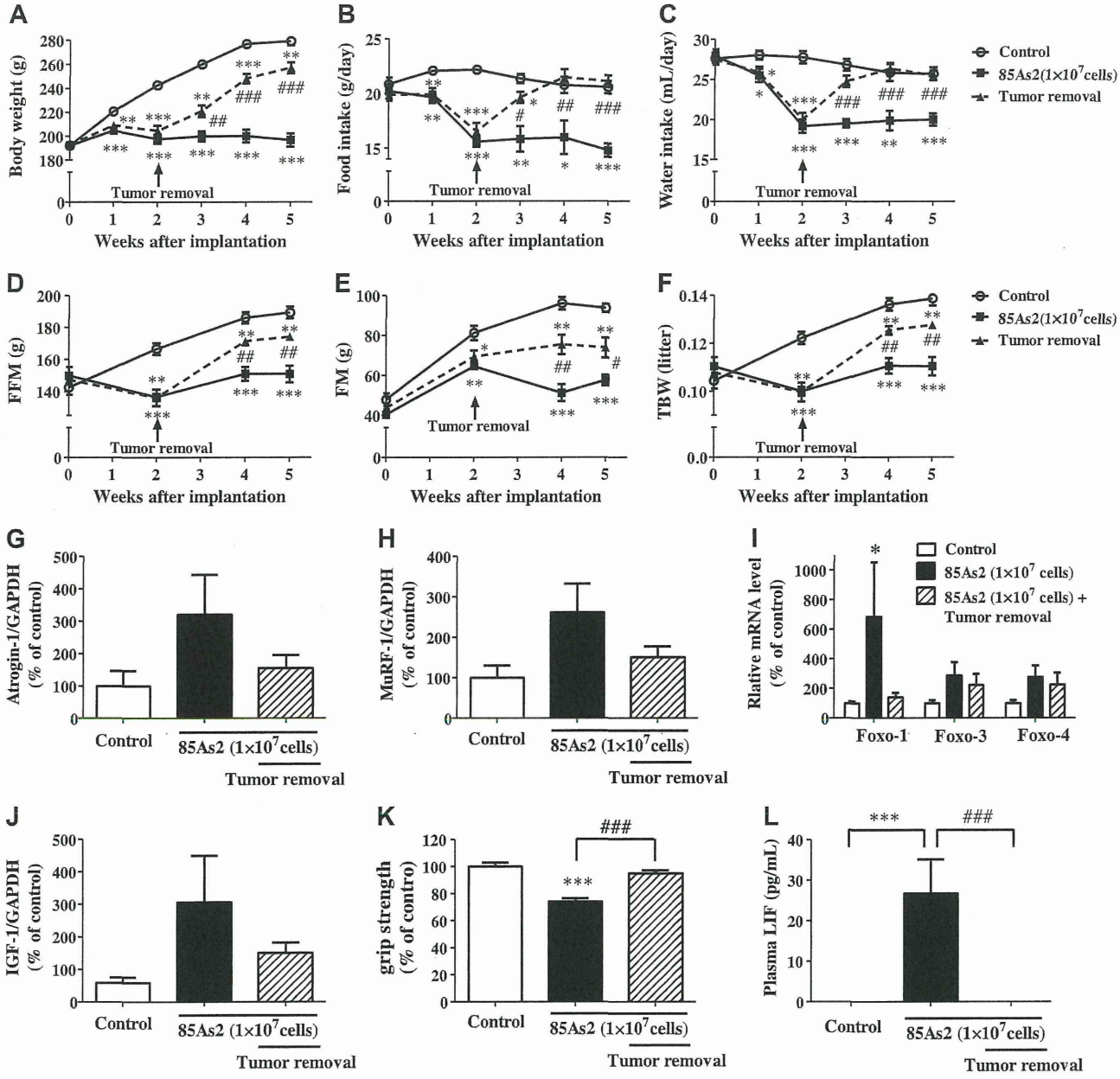

Fig. 5. Effects of tumor removal on body weight (*A*), food intake (*B*), water intake (*C*), FFM (*D*), FM (*E*), TBW (*F*), atrogin-1 (*G*), MuRF-1 (*H*), forkhead box O (*Foxo*; *I*), insulin-like growth factor-1 (*IGF-1*; *J*), grip strength (*K*), and plasma leukemia inhibitory factor (LIF; *L*) levels in nude rats implanted with 85As2 cells (1×10^7 cells/each site) or saline (control) in both flanks at *week 0*. Plasma and the gastrocnemius muscle of the rats were collected 5 wk after implantation. Each data point or bar represents the mean ± SE of 8–9 rats (*A–C*, *K*, and *L*). Each data point or bar represents the mean ± SE of 5 rats (*D–J*). Differences between groups were evaluated using Student's *t*-test or the Mann-Whitney *U*-test. Differences in plasma LIF levels between groups were evaluated using the Kruskal-Wallis test, followed by post hoc Dunn's multiple comparison test. $^{*}P < 0.05$, $^{**}P < 0.01$, and $^{***}P < 0.001$ vs. the control group; $\#P < 0.05$, $\#\#P < 0.01$, and $\#\#\#P < 0.001$ vs. the corresponding 85As2 group.

were significantly reduced in cachectic rats at 12 wk after implantation compared with control rats (Fig. 1*F*). Symptoms of cancer cachexia, including weight loss, low FM and FFM, and wasting of muscle and adipose tissues, were more pronounced in the 85As2 group than in the MKN45cl85 group.

85As2-induced cancer cachexia rat model characterization. Because the 85As2 model induced more severe cancer cachexia in rats than the MKN45cl85 model, the 85As2-induced cancer cachexia model was characterized further. Tumor volume grew progressively in a cell concentration-dependent manner, reaching 1.94 ± 0.57 and 4.38 ± 0.68 cm^3 at 4 wk after implantation of 1×10^6 and 1×10^7 85As2 cells, respectively (Fig. 2*B*). The body weight of the control group continued to increase during the experiment, whereas the body weight of the 85As2 groups did not. Body weight loss was higher in the 85As2 groups than in the control group beginning

Table 2. *Plasma levels of human cytokines in the cancer cachexia rat models and cell culture supernatants*

Time after Inoculation	Cells	IL-1β	IL-6	IL-8	TNFα	LIF
Plasma (2 wk)						
Control		<2.44	<2.44	<2.44	<2.44	<2.44
85As2	1×10^6	<2.44	<2.44	<2.44	<2.44	5.35 ± 3.49
MKN45cl85	1×10^7	<2.44	<2.44	<2.44	<2.44	12.94 ± 2.02*
Plasma (4 wk)						
Control		<2.44	<2.44	<2.44	<2.44	<2.44
85As2	1×10^6	<2.44	<2.44	<2.44	<2.44	24.38 ± 5.99
MKN45cl85	1×10^7	<2.44	<2.44	<2.44	<2.44	41.77 ± 11.08*
Plasma (12 wk)						
Control		<2.44	<2.44	<2.44	<2.44	<2.44
85As2	1×10^7	<2.44	<2.44	39.88 ± 25.14**	<2.44	321.18 ± 42.02**
MKN45cl85	1×10^7	<2.44	<2.44	<2.44	<2.44	75.78 ± 17.51
Supernatant (24 h)						
85As2	5×10^5	ND	ND	10.36 ± 0.70***	ND	611.74 ± 3.84**
MKN45cl85	5×10^5	ND	ND	321.47 ± 22.98	ND	416.00 ± 26.71
Supernatant (48 h)						
85As2	5×10^5	ND	ND	19.02 ± 3.93***	ND	937.29 ± 18.48**
MKN45cl85	5×10^5	ND	ND	559.98 ± 25.16	ND	724.91 ± 22.50

Cytokine levels in cell culture supernatants are expressed as the mean ± SE of triplicate wells in pg/ml, and plasma cytokine levels are expressed as the mean ± SE (pg/ml) values for 4–5 rats. LIF, leukemia inhibitory factor; ND, not detectable (below the minimum detection limit of the assay). Rats were implanted subcutaneously with MKN45cl85 or 85As2 cells (1×10^6 or 10^7 cells/site) or saline alone in both flanks. Differences in plasma cytokine levels between groups were evaluated using the Kruskal-Wallis test, followed by a post hoc Dunn's multiple comparison test (*$P < 0.05$ and **$P < 0.01$ vs. the corresponding control group). Supernatants were collected from 24- or 48-h incubation cultures. Differences in the cytokine levels in cell culture supernatants for the groups were evaluated using Student's *t*-test (**$P < 0.01$ and ***$P < 0.001$ vs. the corresponding MKN45cl85 group).

at 2 wk after implantation and became significant at 3 and 2 wk after implantation of 1×10^6 and 1×10^7 cells, respectively (Fig. 2*A*). The differences in body weight between the 85As2-implanted groups and corresponding control groups were greatest at 4 wk after implantation. The differences in body weight between the 85As2 groups and control group were 70.1–74.3 and 82.7–84.7% regardless of body weight with or without the tumor weight at 4 wk after implantation of 1×10^7

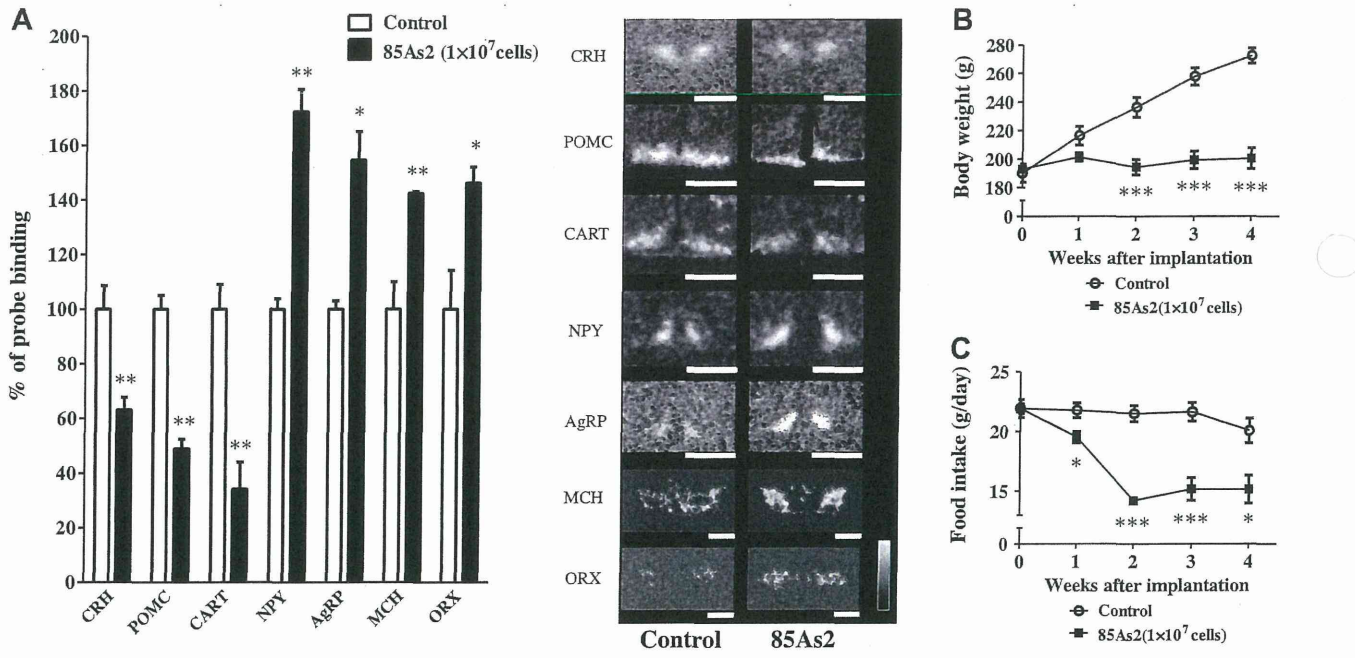

Fig. 6. *A*: mRNA expression of neuropeptide Y (*NPY*), agouti-related protein (*AgRP*), proopiomelanocortin (*POMC*), and cocaine- and amphetamine-regulated transcript (*CART*) in the arcuate nucleus (ARC), corticotropin-releasing hormone (*CRH*) in the paraventricular nucleus (PVN), and orexin (*ORX*) and melanin-concentrating hormone (*MCH*) in the lateral hypothalamic area (LHA) in control and 85As2-induced cachectic rats 4 wk after implantation. Nude rats were inoculated subcutaneously with 85As2 cells (1×10^7 cells/each site) or saline (control) in both flanks at *week 0*. In situ hybridization was measured 4 wk after implantation. Representative autoradiographs of sections hybridized by a ^{35}S-labeled oligodeoxynucleotide probe complementary to mRNA for all the peptides mentioned in *A*. Signal intensity ranges from high (black bars) to low (open bars). Black bar = 1 mm. *B* and *C*: time course changes in body weight (*B*) and food intake (*C*). Changes in body weight and food intake were evident at 4 wk after implantation. Each bar or data point represents the mean ± SE of 6 rats. Differences between groups were evaluated using Student's *t*-test. *$P < 0.05$, **$P < 0.01$, and ***$P < 0.001$vs. the control group.

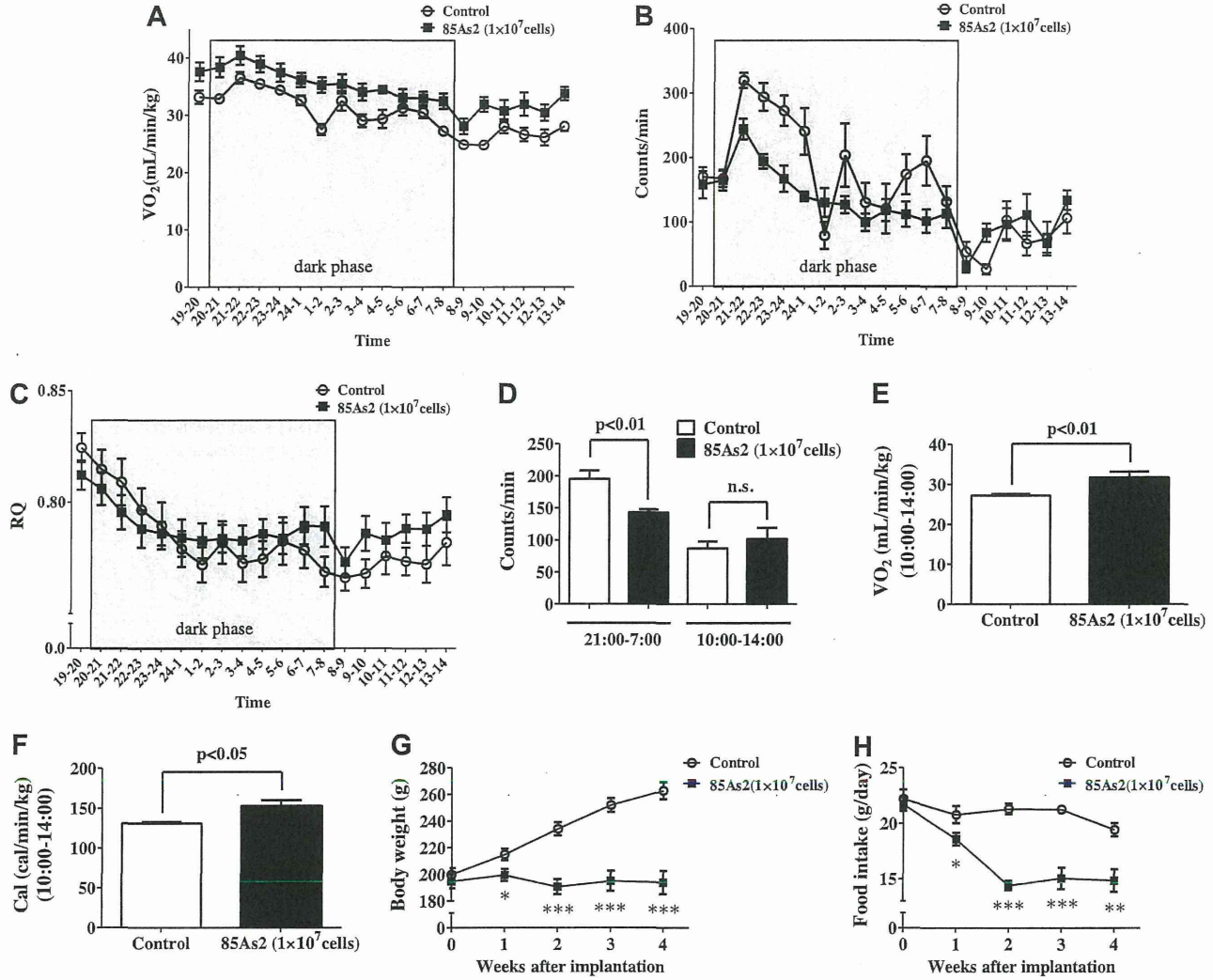

Fig. 7. Time course changes in oxygen consumption ($\dot{V}O_2$, ml·min^{-1}·kg^{-1}; *A*), locomotor activity (*B*), respiratory quotient (RQ; *C*), average cumulative locomotor activity (*D*), $\bar{V}O_2$ (ml·min^{-1}·kg^{-1}) (*E*), and metabolic calories (cal·min^{-1}·kg^{-1}; *F*) from 1000 to 1400 at 4 wk after 85As2 cell implantation in nude rats. Rats were inoculated sc with 85As2 cells (1×10^7 cells/each site) or saline (control) in both flanks at *week 0*. Respiratory metabolism was measured 4 wk after implantation. Changes in body weight (*G*) and food intake (*H*) over time. Changes in body weight and food intake were evident at 4 wk after implantation. Each data point or bar represents the mean ± SE of 7 rats. Differences between groups were evaluated using Student's *t*-test or the Mann-Whitney *U*-test. $*P < 0.05$, $**P < 0.01$, and $***P < 0.001$ vs. the control group.

and 1×10^6 cells, respectively (Table 1). Comparison between peak body weight and body weight 4 wk after implantation showed body weight loss in each cachectic rat (1×10^7 cells, 88.0 ± 3.5%; and 1×10^6 cells, 94.4 ± 2.7%). These comparisons were made using the corresponding individual peak body weight. All body composition parameters (FFM, FM, and TBW) were also substantially lower in the 85As2 groups than in the control groups (Fig. 2, *E–G*).

Reductions in food and water intake were observed beginning at 1 wk after implantation in the 85As2 groups compared with the corresponding control groups and became significant 2–4 wk later (food intake: 1×10^7 cells, 73.5–78.7%; and 1×10^6 cells, 89.0–90.7%; water intake: 1×10^7 cells, 71.2–80.1%; and 1×10^6 cells, 83.4–88.7%; Fig. 2, *C* and *D*). Similarly to the 85As2-induced cachexia model, MKN45cl85-implanted rats also exhibited marked decreases in food intake (Fig. 2*H*). However, the decrease in food intake was less pronounced in MKN45cl85-implanted rats than in 85As2-implanted rats (MKN45cl85, 1×10^7 cells, 83.8–87.0% compared with the corresponding control groups).

Muscle (greater pectoral, gastrocnemius, tibialis, and soleus), adipose tissue (epididymal, perirenal, and mesentery fat), liver, and spleen weights decreased substantially in a cell concentration-dependent manner at 4 wk after implantation in cachectic rats compared with that in control rats (Table 1). Macroscopic and histological observations confirmed gastrocnemius muscle atrophy in the 85As2 group (1×10^7 cells) at 4 wk after implantation (Fig. 3, *A–C*). Furthermore, all cells in Fig. 3, *B* and *C* (control, $n = 51$; 85As2, $n = 75$), were measured, and the cross-sectional area, perimeter, Feret diameter, and minimum Feret diameter were calculated. The cross-sectional area (1,460.4 ± 76.3 vs. 2,023.9 ± 85.2 μm^2, $P <$